Closed Loop ^{3}He JT Stage Performance Demonstration

W Chen[1], B Moore[1], and The PRIMA Study Team

[1] Jet Propulsion Laboratory, California Institute of Technology, Pasadena, California

Email: weibo.chen@jpl.nasa.gov

Abstract. To advance the cryocooling system for the PRobe far-Infrared Mission for Astrophysics (PRIMA) mission concept, a closed-loop JT stage was assembled using flight-like residual hardware from the JWST program. The system was tested to assess its cooling capacity at 4.5 K and to evaluate compressor stability across the design heat sink temperature range. The performance of the JT stage was characterized over a range of cooling temperatures, precooling temperatures, and heat sink temperatures. This paper presents test results obtained without applying a DC current to maintain the piston dynamic center position. The maximum piston stroke was determined experimentally to verify adequate forward headroom across the full expected operating temperature range. Measured performance is compared with both predicted values and the capability requirements for the PRIMA mission.

1. Background

1.1 PRIMA mission

The PRobe far-Infrared Mission for Astrophysics (PRIMA) is a NASA cryogenic observatory designed to operate in a halo orbit around Earth–Sun L2 point. It is intended to address fundamental questions about our cosmic origins by investigating the role of water in planet formation, the co-evolution of galaxies and their supermassive black holes, and the evolving properties of dust and metallic elements over cosmic time (Bradford et al., 2022). The telescope's 4.5 K operating temperature is required to ensure that thermal emission from the telescope contributes no more than 25% of the natural background at the longest wavelengths accessible to the instruments. The instrument optics are maintained near 1.0 K to minimize thermal emission through a stack of two focal plane filters. The focal plane detectors are maintained at 0.12 K to enable kinetic inductance detector (KID) sensitivity.

To efficiently cool key components to their target operating temperatures, a hybrid passive and active cooling system has been selected for the PRIMA mission, as illustrated in Figure 1 (Chen et al., 2023). The multi-stage passive cooling system, located between the payload enclosure and the spacecraft sunshade and bus, reduces parasitic radiative loads on the cryogenic payload. This passive design draws heritage from the Spitzer, Herschel, and NEO Surveyor observatories. The three-stage passive system reduces the temperature of the shields adjacent to the actively cooled stage to approximately 45 K. Active cooling then provides additional temperature reduction from 18 K down to 0.12 K. The active system includes a mechanical cryocooler—based on the JWST MIRI cooler—that delivers cooling at

18 K and 4.5 K, and a Continuous Adiabatic Demagnetization Refrigerator (CADR), adapted from the XRISM ADR system, that provides cooling at 1 K and 0.12 K.

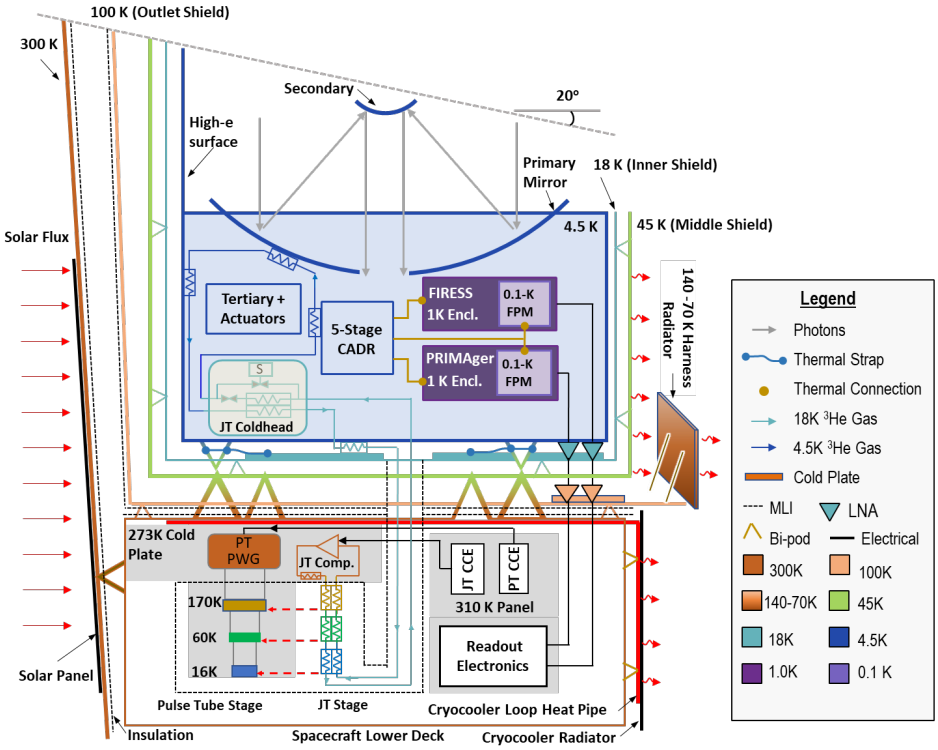

Figure 1. PRIMA payload thermal block diagram. The Sun and Earth are located to the left, science targets are oriented toward the top, and deep space is to the right

1.2 Prima baseline JT stage

Based on the predicted margined heat loads at 18 K and 4.5 K, the required cooling capacities of the cryocooler are 235 mW and 53 mW, respectively. No existing flight-qualified cryocooler operating at 4.5 K is capable of meeting this cooling requirement. Due to budgetary and schedule constraints, the PRIMA flight cooler must be based on existing flight-proven subsystems and component hardware technologies, minimizing the need for new hardware development. To this end, the PRIMA mission design team has focused on modifying the spare flight cooler developed for JWST's MIRI instrument to deliver more than 50 mW of cooling at 4.5 K. PRIMA's hybrid cooler uses ^{3}He instead of ^{4}He as the working fluid in the JT stage. The use of ^{3}He enables a JT restriction outlet pressure of approximately 2.4 bar—about twice that of a JT stage using ^{4}He. This higher outlet pressure permits a significantly higher compressor suction pressure, which increases both the system mass flow rate and the specific cooling capacity via the JT effect, while maintaining a fixed compression ratio compatible with a single-stage compression system.

1.3 Previous compressor performance demonstration with ^{3}He

A flight-like demonstration model (DM) compressor was previously shown to achieve the required mass flow rate for the JT stage at the target pressure ratio of 3.3, with an inlet pressure of 2.4 bar (Chen et al., 2023). During these tests, the piston stroke length was maintained at 64% of its maximum value, and the piston DC position was held near the neutral (idle) point. The compressor's AC input power remained slightly below 70 W while delivering the required mass flow rate for the JT stage, with an inlet temperature of 301 K—higher than the design inlet temperature of 273 K. These results suggest that a

single MIRI JT compressor may be sufficient to meet the PRIMA JT stage requirements, potentially eliminating the need for the second compressor in the original baseline design.

The DM compressor performance demonstration was conducted with the piston's dynamic center maintained very close to its static center. This was achieved by regulating the piston back pressure via control of the back-pressure bleed flow rate using a needle valve, while monitoring the piston position with a displacement probe.

2. Valved linear compressor piston dynamic center offset

2.1 Background on piston dynamic center (PDC) offset

All current aerospace linear compressors use flexure-supported pistons with clearance seals between the piston and cylinder to eliminate mechanical wear, enabling operating lifetimes exceeding 10 years (Figure 2). In these compressors, the dynamic center of each flexure-supported piston can shift axially in response to changes in the differential pressure across the piston. In contrast, the center of a piston driven by a conventional crankshaft remains fixed and does not drift.

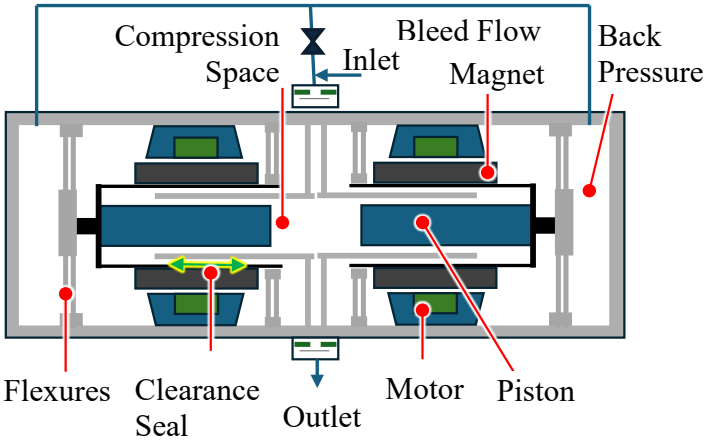

Figure 2. Schematic of existing linear valved compressor with external bleed valve

The instantaneous mass flow rate leaking across the piston clearance seal is not a linear function of the differential pressure across the piston, as it also depends on the local gas density, which is proportional to the gas pressure within the seal. If the piston backpressure equals the time-averaged pressure in the compression chamber, the integrated mass flow leaking to the back side of the piston over a cycle will exceed the mass flow leaking out. This imbalance causes the backpressure to rise until inflow and outflow in the back chamber are equalized. The resulting increase in backpressure displaces the piston toward top dead center (TDC) at the fore end of the cylinder, reducing the usable piston stroke and thereby degrading compressor performance.

2.2 Bleed flow to reduce PDC offset

Current compressors, including the JWST MIRI compressor, mitigate this issue by bleeding gas from the back volume to the suction port through an external fixed orifice, thereby reducing the back pressure to match the effective pressure in the compression chamber. However, this simple approach is effective only when the compressor operates at a specific temperature and pressure, as the seal leak rate can vary significantly with changes in operating conditions. The gap between the piston and cylinder is very narrow—typically less than 10 micrometers—to reduce the leak rate across the seal. Consequently, this gap can change by a large percentage due to the coefficient of thermal expansion (CTE) mismatch between the piston and cylinder as the temperature varies. Significant variations in leak rate can substantially alter the back pressure, and thus the PDC.

2.3 PDC offset control challenges for PRIMA

To mitigate PDC drift, many valved linear compressors—including the MIRI JT compressor—apply a prescribed DC current to the linear motor to generate an offsetting force that counteracts the pressure force. The direction and amplitude of this DC current are typically determined using piston position sensors. A series of tests at various heat sink temperatures and pressures is typically performed to establish the correlation between the required DC current and piston centering. In the MIRI Flight-Spare (FS) compressor, however, the position sensor was removed prior to the final housing assembly.

The correlation developed for the MIRI application is not applicable to PRIMA due to significant differences in working fluid and compressor operating conditions. To update the DC current control parameters for adapting the MIRI FS compressor to PRIMA, it would be necessary to modify the JT compressor housing to reinstall a position sensor and conduct a series of tests to determine the DC current required to center the pistons under varying operating conditions and control inputs. The resulting test data would then be used to update the control model. This approach would entail substantial effort, including hardware modification, extensive testing, compressor reassembly, and requalification of the JT compressor for flight.

2.4 Modify flow impedance to achieve back pressure that centers piston

To avoid these complex procedures, we plan to restrict the heat sink temperature range to a narrow band of 268–278 K, thereby minimizing PDC offset drift over this range. In addition, the flow impedance in the bleed flow path will be modified to help maintain the PDC near the static center under nominal operating conditions.

The piston dynamic offset is directly proportional to the force imbalance between the cycle-averaged pressures acting on the forward and aft faces of the piston, and inversely proportional to the spring stiffness. These parameters do not vary between units of the same design. It is important to note that although the clearance seal leak rate can vary substantially between compressors, such differences should not affect the PDC, provided that the piston back pressure and the compression volume pressures are the same. Thus, a back pressure that centers the piston in the DM compressor should also center it in the FS compressor, assuming identical operating pressures and equivalent cycle-averaged pressures on the piston's forward face.

The DM compressor is equipped with a piston position sensor, allowing straightforward determination of the back pressure required to center its PDC.

2.5 Estimate piston position during cooldown

During the cooldown process, system pressures can be significantly higher than the steady-state operating pressures, and the clearance seal leak rate can also exceed that observed during steady-state operation. This may cause the PDC to drift significantly forward. Accurate knowledge of the PDC is essential for maximizing piston stroke length to increase cooling power while avoiding piston-to-head contact (knocking). Enhancing cooling power is particularly critical during the JT stage pinch-point crossing to ensure that the available cooling capacity exceeds parasitic loads.

The pressure on the piston's forward face varies between the maximum and minimum values in the compression chamber. The time-averaged pressure on the forward face can be significantly lower than the arithmetic mean of the maximum and minimum pressures due to the rapid pressure rise and fall near the peak. The effective pressure on the forward face can be inferred from the back pressure required to center the PDC. A correlation can be established between this effective pressure in the forward chamber and the compressor's inlet and outlet pressures over the wide pressure range expected during the cooldown process. With this correlation, along with knowledge of the back pressure and piston stiffness, the PDC during cooldown can be estimated.

3. Closed loop JT stage performance with ^{3}He at 4.5 K

3.1 Test facility

To measure the ^{3}He JT stage performance using the MIRI flight spare hardware, assess the JT compressor PDC stability over a narrow heat sink temperature range, and develop a correlation for the forward pressure, a test loop—comprising a flight-like JT compressor, a Heat Exchanger Stage Assembly (HSA), and Ground Support Equipment (GSE)—was assembled, as shown in Figure 3 and Figure 4. The HSA consists of a JT recuperator, a JT throttle, a bypass valve and an external enclosure supported by a set of bipods. A commercial GM pulse tube cooler precools the JT high-pressure stream below 18 K, simulating the flight pulse tube precooler, while a simple tube-in-tube GSE recuperator reduced the heat load on GM pulse-tube. The throttling valves at the warm end of this recuperator controls the flow pressures at the warm end of the HSA to values predicted by the JT analysis model.

Additionally, a two-stage GM cold-head cools a two-stage shroud, minimizing parasitic heat loads on the HSA and load simulator heat exchangers. The DM compressor is nearly identical to the flight compressor, but includes a piston position sensor—absent in the Flight Model (FM)—which measures the piston's dynamic position under various operating conditions to determine stroke headroom. To allow operation below the ambient dew point, the DM compressor is housed inside a bell bar at a rough vacuum pressure to prevent condensation. A ^{3}He fill and recovery cart with a cryogen sorption pump boosts ^{3}He pressure from a low-pressure supply bottle and recovers the ^{3}He in the test facility.

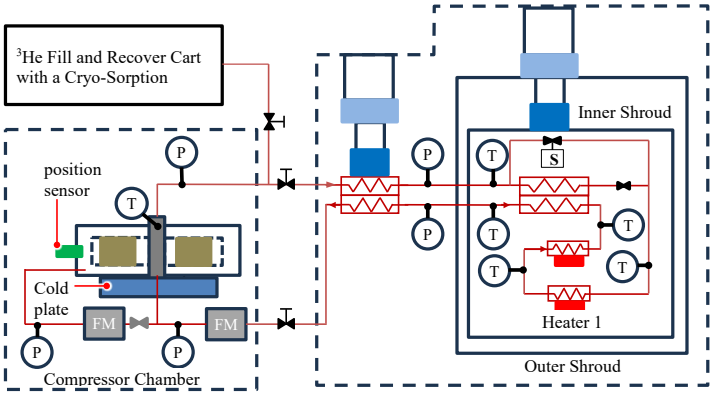

Figure 3. Schematic of He^3 JT stage test facility (axillary components such as accumulators, getter, safety relief valves are not shown for clarity)

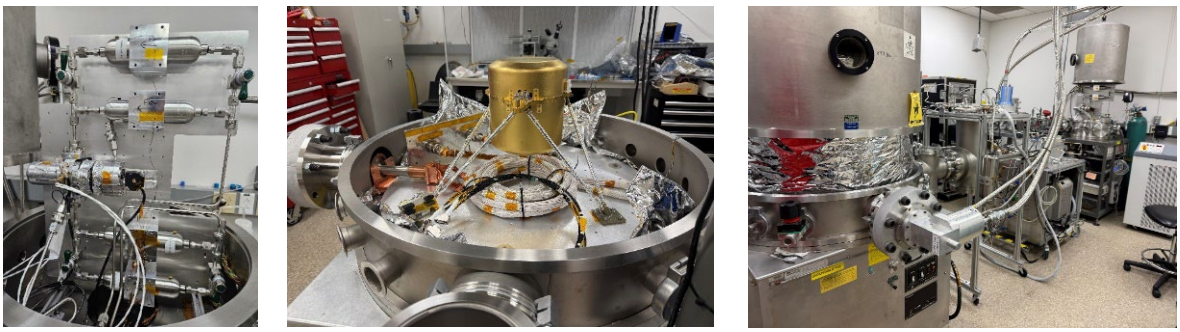

(a) JT Compressor in Vacuum Chamber (b) HSA before Thermal Shroud Installation (c) Overall Test Facility

Figure 4. Closed-loop ^{3}He JT stage test facility using MIRI DM compressor and HSA

3.2 Test results

A series of shakedown tests with ^{4}He was carried out after the vacuum chamber was evacuated and the temperature of the inner cooling shroud reached its final temperature of approximately 22 K. These tests included JT stage pinch point crossing and measurement of parasitic heat leaks at the cold end. Upon

completion, the system was evacuated and charged with ^{3}He, with the cryo-sorption pump used to boost the supply source pressure. The JT stage cooling capacity was measured across a range of cooling temperatures, precooling temperatures, and slight variations in inlet and outlet pressures. In addition, the impact of heat sink temperature variation on both the JT stage cooling power and the compressor piston dynamic center (PDC) offset was evaluated at different flow rates. A correlation was then developed between the effective pressure force acting on the piston's forward face and the compressor operating pressures. This correlated pressure, together with the measured back pressure, was used to predict the PDC, and the prediction approach was subsequently validated.

3.2.1. Effect of precooling and cooling temperatures on JT cooling power

The ^{3}He JT stage achieves a net cooling power exceeding 45 mW under nominal design conditions, as shown in Figure 5. In these tests, the JT stage precooling temperature and the temperature of the flow returning to HSA were regulated using heaters controlled by standard Lakeshore controllers. The measured heater power at 4.5 K corresponds to the net cooling power. This value does not include the estimated parasitic heat load into the JT cold end, which is approximately 6.7-6.9 mW, as discussed in Section 3.2.3. The JT stage cooling power was observed to decrease with increasing precooling temperature and with decreasing cold-end temperature, consistent with thermodynamic expectations. The AC input power to the JT compressor during these tests was 62.8 W.

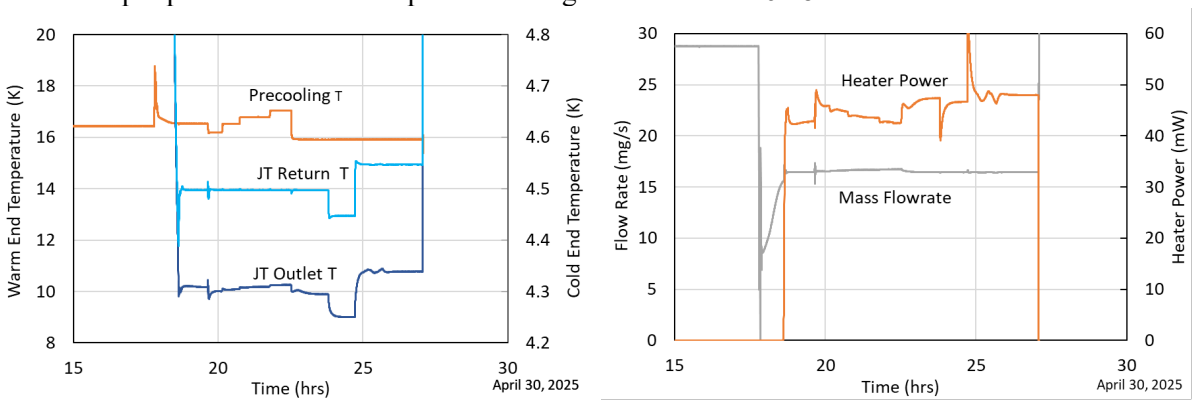

Figure 5. Temperatures of JT flow exiting capillary tube and flow returning to HSA recuperator at different precooling and cold end temperatures

3.2.2. *Effects of heat sink temperature on cooling power and piston stroke margin*

During flight operations, the effective heat sink temperature of the cryocooler compressor may fluctuate slightly due to minor variations in the solar thermal load on the observatory. This temperature is expected to remain within a limited range of 268–278 K. The cooling power increases by 1.3 mW as the sink temperature decreases from 273 K to 268 K, and decreases by 1.7 mW as it rises to 278 K.

Within this heat sink temperature range, the compressor PDC remained highly stable as shown in Figure 7. Although no DC current offset was applied in the compressor drive to actively control the PDC, the piston position drift was minimal. Importantly, the minimum piston forward headroom remains above the minimum allowable value specified for the MIRI application. This held true even under operating conditions that required higher mass flow rates to achieve increased cooling power (see Table 1.in Section 3.4 for additional details). In fact, the minimum headroom is very close to that observed during pinch-point crossing in the MIRI configuration. These results suggest that compressor operation in the PRIMA application will maintain a similar safety margin against piston knocking.

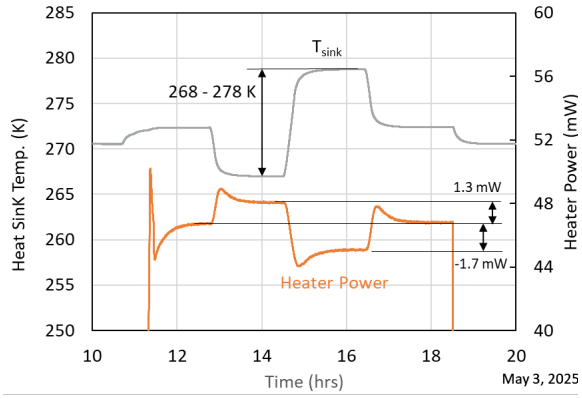

(a) Heat Sink Temperature and Cooling Power

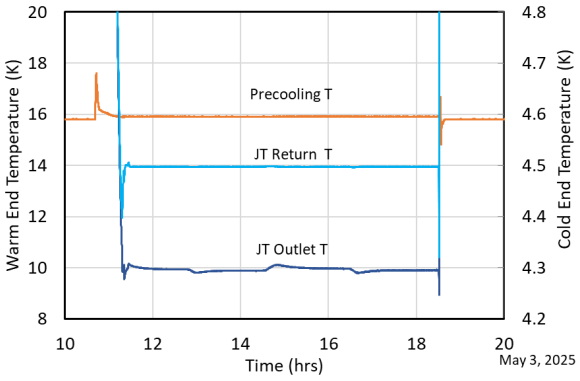

(b) Cooling and Precooling Temperatures

Figure 6. JT stage cooling power and cold end temperature as heat sink temperature varies

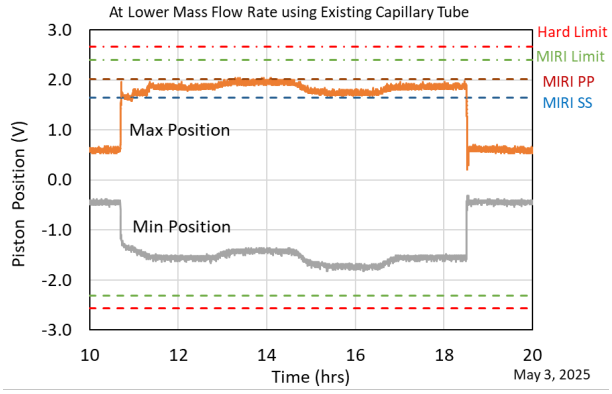

(a) Mass flow rate of 16.5 mg/s

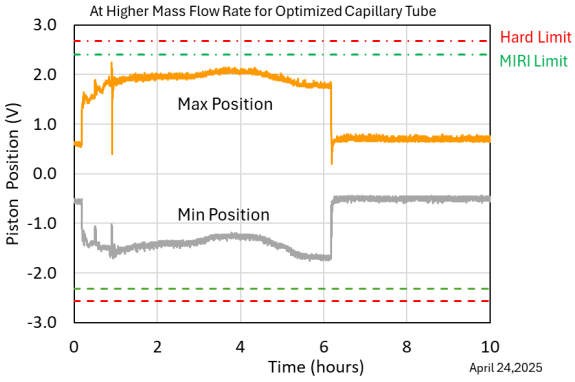

(b) Mass flow rate of 20.7 mg/s

Figure 7. Piston dynamic position and stroke margin (a) Piston position as heat sink temperature varies. (b) Piston position at a higher flow rate for the optimized JT capillary tube.

3.2.3. Parasitic load on JT cold end

With a fixed parasitic load, the temperature rise across the cold end is inversely proportional to the flow heat capacity (i.e., $\propto 1/(\dot{m}\, c_p)$). When the flow heat capacity is infinitely large (i.e., $1/(\dot{m}\, c_p) = 0$), the temperature rise should be zero, and the difference between the outlet and inlet temperature sensor readings corresponds to the sensor offset. Figure 8 shows the flow temperature rise across the load simulators as a function of mass flow rate, with the heaters on the simulators turned off.

The slopes of the trend lines in Figure 8, which relate $1/(\dot{m}\, c_p)$ to temperature rise, suggest that the parasitic load on the cold end is approximately 6.9 mW with ^{3}He when the cold end is between 4.5 K and 6.0 K. The inferred temperature sensor offset is approximately - 11 mK. The parasitic load deduced from the ^{3}He test data is consistent with results obtained using ^{4}He.

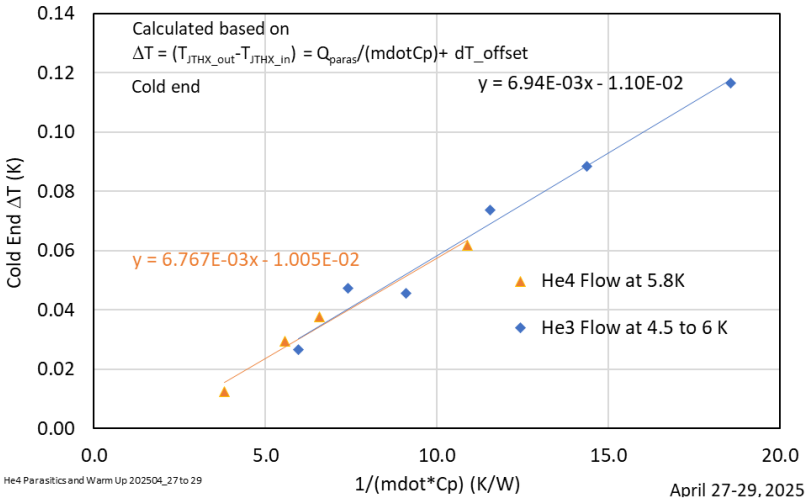

Figure 8. Temperature differential across cold-end load simulator vs. flow heat capacity

3.3 Piston dynamic center estimate

We determined the cycle-averaged pressure on the forward face of the piston based on the piston backpressure and the pressure force difference inferred from the measured PDC offset. This average pressure was then correlated with the compressor inlet and outlet pressures. Using this correlation, we predicted the piston DC offset and found good agreement between the predicted and measured values, providing confidence in this approach for estimating the PDC offset of the MIRI FS compressor.

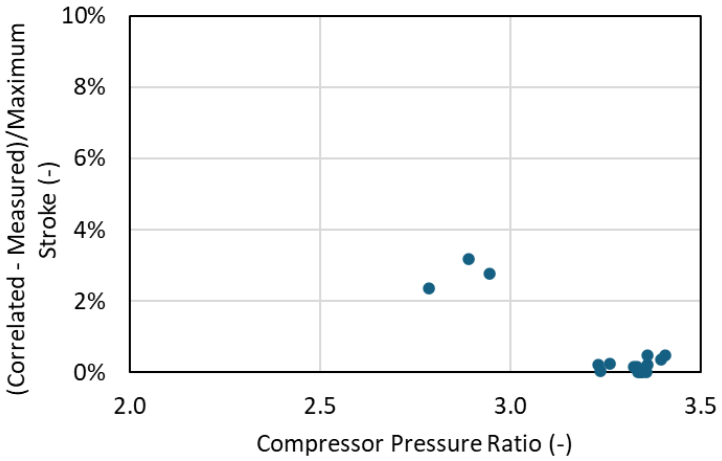

Figure 9. Predicted PDC based on correlated cycle-averaged pressure on the piston's forward face. The heat sink temperatures are 295 K and 273 K.

3.4 Discussions

The JT stage test condition closely matches the design specification, as shown in Table 1. The measured net cooling power is 45.8 mW. When accounting for the parasitic load credit, the effective cooling power increases to 52.7 mW. As the sink temperature rises to 278 K, the cooling power decreases slightly to 50.8 mW.

Table 1. MIRI flight-like JT stage performance with ^{3}He and PRIMA cooler operating conditions

Cases		T_{sink} (K)	$P_{Low, comp}$ (bar)	$P_{High, comp}$ (bar)	$T_{precool}$ (K)	$T_{c—JT}$ (K)	Q_{JT} (K) (mW)	Flow Rate (mg/s)
Existing JT Restriction	Analysis	275.0	2.448	8.152	16.21	4.5	48.7	16.58
	Measured Values	272.4	2.36	7.92	16.18	4.497	45.8 (+6.9)	16.45
Opt. JT Restriction*	Analysis	275.0	2.443	8.135	16.66	4.5	52.8	20.66*
*The mass flow rate with optimized JT restriction is used as the requirement for the compressor								

The measured cooling power with ^{3}He is consistent with the predicted cooling power from REFPROP, as shown in Figure 10. The vertical offset between the green dashed line and the reference line represents the average parasitic load measured at the JT cold end, as discussed in Section 3.2.3. The predicted power is derived from a JT model. This model assumes a differential temperature between the flow streams at the cold end of the HSA recuperator, as defined by a correlated model for the MIRI system. All data points lie above the green dashed line, indicating that the predicted cooling power is slightly higher than the measured values adjusted for parasitic heat loads. Agreement diverges slightly at higher cooling powers when the JT precooling temperatures are reduced. This likely occurs because the test cooling capacity becomes limited by enthalpy differences at the cold end, whereas the JT model, based on predicted fluid properties, still considers the capacities limited by enthalpy differences at the warm end (see the next paragraph for further discussion). This discrepancy is not unexpected, as fluid temperatures near the critical point introduce large uncertainties in predicted non-ideal fluid properties.

Figure 11 presents the predicted enthalpy differences between the low- and high-pressure streams from REFPROP (Lemmon, 2023) and He3Pak (v2.0), along with a reference line representing the measured specific cooling enthalpy. For a JT stage operating at optimal pressures, the flow-stream enthalpy differences at the precooling and cooling stages should closely match. The maximum specific cooling enthalpy (i.e., cooling power per unit mass flow rate) is constrained by the minimum enthalpy difference. Losses due to the limited thermal effectiveness of the recuperator further reduce the specific cooling enthalpy. The measured cooling enthalpy agrees well with the predicted enthalpy difference, suggesting that the system pressure is near optimal and the recuperator losses are minimal. Because the enthalpy difference at the cold end is highly temperature-dependent, the predicted JT stage performance becomes sensitive to uncertainties in the predicted fluid properties—especially when the cold-end enthalpy difference limits system performance.

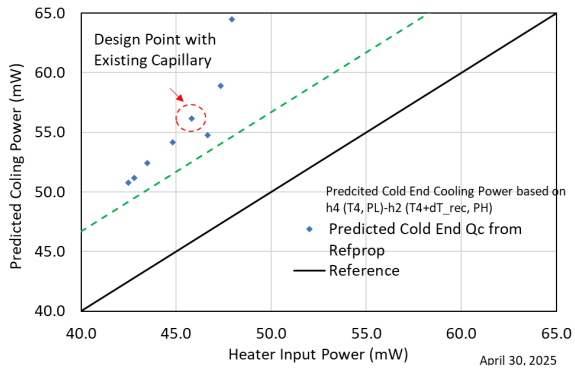

Figure 10. Comparison between Measured and Predicted Cooling Power

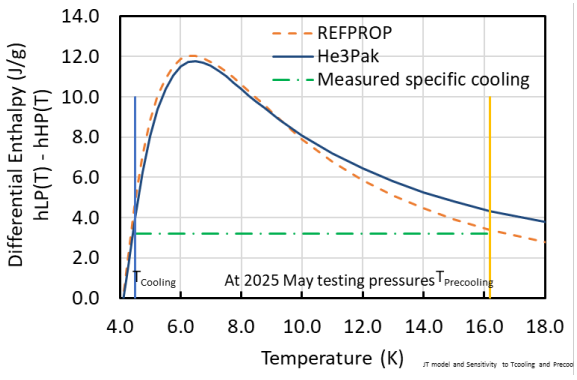

Figure 11. Predicted Differential Enthalpy between Low- and High-Pressure Streams across Warm-to-Cold End Temperatures

4. Conclusions

Using flight-like compressor and HSA, testing has demonstrated that the modified MIRI cooler achieves a net cooling power exceeding 45 mW at 4.5 K. Taking into account the estimated 6.9 mW parasitic load into the JT cold end, the actual cooling power of the JT stage is about 51.9 mW. The JT compressor is capable of delivering a higher flow rate while maintaining the same inlet and outlet pressures. Additionally, using a less restrictive capillary tube could further enhance the net cooling performance. This demonstrated capability supports the expectation that the PRIMA thermal system can maintain both the 18 K and 4.5 K temperature stages at their operating conditions with a 100% heat load margin, as required at the concept study stage. Moreover, the compressor piston stroke length and available headroom remain comparable to those of the MIRI system during pinch-point crossing and are within the safe operating range—even when operating at a higher flow rate with the modified capillary. Finally, the piston position has been observed to correlate with the pressures in the back volume, as well as at the inlet and outlet, providing valuable diagnostic information for system performance.

Acknowledgments

The authors acknowledge the late Michael Petach of Northrop Grumman Space Systems, who passed away in June 2024. His insight into the MIRI cryocooler system was invaluable during the early phases of the PRIMA cryocooler design study.

The research was carried out at the Jet Propulsion Laboratory, California Institute of Technology, under a contract with the National Aeronautics and Space Administration.

References

[1] Bradford C, et. al., 2022 “The PRIMA Far-Infrared Probe: Observatory and Instrumentation”, American Astronomical Society Meeting Abstracts, Vol. 54, No. 6.
[2] Chen, W., Moore, B. D., DiPirro, M. J., Shirron, P. J., & Petach, M. B. (2023). PRIMA space telescope cryocooling system. Proceedings of SPIE, 12687, Infrared Sensors, Devices, and Applications XIII, 1268705. https://doi.org/10.1117/12.2675697
[3] Chen, W., Moore, B., Petach, M., & The PRIMA Team. (2024). Effects of working fluid on performance of 4.5 K JT cooler. IOP Conference Series: Materials Science and Engineering. Presented at the CEC Conference, Honolulu, HI, 2023.
[4] He3Pak 2.0 Distributed by Horizon Techologies Engineering Software & Service
[5] Lemmon E, Private Communications for REFPROP Helium-3 Fluid File (Version 8), 2023